Structural evolution of Co/Cu nanostructures under 1 MeV ion-beam irradiation

M. Cai
Département de physique et Groupe de Recherche en Physique et Technologie des Couches Minces, Université de Montréal, C.P. 6128, Succursale Centre-Ville, Montréal, QC H3C 3J7, Canada

T. Veres
Département de physique et Groupe de Recherche en Physique et Technologie des Couches Minces, Université de Montréal, C.P. 6128, Succursale Centre-Ville, Montréal, QC H3C 3J7, Canada and NRC, Industrial Materials Institute, National Research Council Canada, 75 de Mortangne Blvd., Boucherville, Quebec J4B 6Y4, Canada

S. Roorda, F. Schiettekatte, and R. W. Cochrane
Département de physique et Groupe de Recherche en Physique et Technologie des Couches Minces, Université de Montréal, C.P. 6128, Succursale Centre-Ville, Montréal, QC H3C 3J7, Canada

(Received 27 May 2003; accepted 30 October 2003)

Co/Cu multilayers with composition wavelength ranging from 2 to 10 nm have been deposited and irradiated at various doses from 1×10^{14} to 3×10^{16} ions/cm^2 using 1 MeV Si^+ ions. The ion-beam-induced variation in structural properties such as interfacial mixing, interface roughness, crystallographic texture, and grain size, are characterized by a variety of x-ray scattering techniques. Irradiating Co/Cu multilayers generate metastable Co–Cu alloys whose electrical and magnetic properties have been found to be very similar to the Co–Cu alloys fabricated by other nonequilibrium methods. Fitting to the low-angle x-ray reflectivity spectra using a standard optical model yields a mixing efficiency comparable to the prediction of a ballistic ion-beam mixing model, and interfacial mixing widths consistent with the values estimated from saturation magnetization measurements. © *2004 American Institute of Physics.* [DOI: 10.1063/1.1636529]

I. INTRODUCTION

Giant magnetoresistance (GMR) in magnetic multilayers[1] has attracted great interest due to their potential for important technical applications such as disk drive read heads. Numerous studies show that GMR is closely related to the scattering of conduction electrons at or near the interfaces in the antiferromagnetic phase.[2] Therefore, interface modification techniques are highly desirable either for the purpose of investigating the origins of GMR or for optimizing GMR in practice. Among the various techniques available, ion-beam irradiation has been proved to be a very effective tool for many GMR multilayer systems, such as Fe/Cr,[3] Fe/Ag,[4] and Cu/Co.[5] In this context, ion irradiation has at least two advantages over other techniques: first, it is able to modify the interface structure of a *single* existing multilayer systematically and controllably; second, the ballistic nature of ion-beam mixing at low temperatures makes it possible to completely mix two elements even in an immiscible system with positive mixing heat.[6]

Co/Cu is the multilayer system revealing the largest GMR at room temperature and, thus, is one of the most suitable candidates for industrial applications. In our previous article,[5] we reported preliminary results of the ion irradiation effects on the GMR and interlayer antiferromagnetic coupling in such multilayers. However, the first step towards correlating such effects to their physical origins is to have a thorough characterization of structure modification upon ion-beam bombardment. Conventional methods to obtain information on ion-beam mixing include Rutherford backscattering spectrometry, secondary ion mass spectrometry, and Auger electron spectroscopy with ion etching. However, the composition wavelength of a GMR multilayer is typically less than 10 nm and significant change in GMR can be associated with angstrom spreads of mixed regions. Probing such subtle mixing effects using the abovementioned methods is usually very difficult, especially for multilayers with little atomic contrast (such as Co/Cu). By contrast, x-ray diffraction techniques offer unique advantages for working at such small scales, including high spatial sensitivity, high penetration, and nondestructive capability. At high angles, x-ray diffraction yields structure information on a crystallographic scale. Ion-beam mixing in textured grains is mainly reflected in the change of relative intensities of superlattice satellite peaks. By fitting such changes, the thickness of ion-beam mixed regions can be determined with angstrom accuracy for many multilayer systems.[7] However, a major difficulty of applying this method to the Co/Cu system lies in that the lattice mismatch between fcc Co (3.54 Å) and fcc Cu (3.61 Å) is less than 2%, which makes the satellite peaks typically very weak and not well defined. On the other hand, at low angles, x-ray reflectivity measurements are sensitive to average modulation profiles of electronic density and absorption coefficient in a multilayer structure, and do not rely on contrast in lattice constant. Despite the fact that Co and Cu elements are very similar in many aspects, our experiments and simulations show that the large contrast in absorption coefficient between Co and Cu provides low-angle x-ray

reflectivity measurements with sufficient sensitivity to detect subtle changes in interface structures of Co/Cu multilayers. Moreover, by modeling the multilayer structure and comparing the calculated x-ray reflectivity spectra of the modeled structures with experimental data, quantitative information about interface modification upon ion irradiation can be obtained.

While the ultimate goal of this work is to have a thorough understanding of the ion-beam irradiation effects on the electrical, transport, and magnetic properties of the Co/Cu multilayers, it is essential to have a quantitative characterization of the structural evolution of the Co/Cu multilayer with a wide range of thickness combinations, under a wide range of ion-irradiation doses. In this article, x-ray scattering techniques and magnetic measurements are applied to investigate this structural evolution. In a subsequent article,[8] the effects of such structural evolution on GMR and magnetic properties will be detailed for the Co/Cu multilayers with large GMR ratios (i.e., $t_{Co} \sim 20$ Å and t_{Cu} near the second ($\sim$22 Å) and the third ($\sim$34 Å) peak of oscillatory antiferromagnetic coupling).

The remainder of this article is organized as follows. In Sec. II, experiment details of sample preparation, ion irradiation, x-ray, and other measurement details are described. In Sec. III, the effects of ion-beam irradiation will be discussed for multilayers with very thin Co layers to examine the possibility of the formation of CoCu alloys and the nature of ion-beam mixing in this system. In Sec. IV, for a multilayer with thick Co and Cu layers, by combining x-ray reflectivity analysis and magnetization measurements, the ion-beam mixing width is estimated as a function of ion dose, and the ion mixing rate is obtained and compared with existing models.

II. EXPERIMENT

Multilayer samples with the configuration $[\mathrm{Co}(x\ \text{Å})/\mathrm{Cu}(y\ \text{Å})]_N$ ($x=5-75$ Å; $y=5-100$ Å; $N=10-50$) were deposited on thermally oxidized Si (100) wafers by rf triode sputtering. Most discussions in the following sections are on a representative multilayer with configuration [Co(50 Å)/Cu(75 Å)]×14, although similar results are obtained for other multilayers with various configurations. In order to simplify the notation, these multilayers are hereafter referred to as $\mathrm{Co}_{50}/\mathrm{Cu}_{75}$. During deposition, the substrate was maintained at 20 ± 3 °C and sputtering was carried out at a rf power of 100 W and an Ar pressure of 3 mTorr, starting from a base pressure before sputtering below 1×10^{-7} Torr. These conditions result in deposition rates of 0.8 and 2.2 Å s^{-1} for Co and Cu, respectively. Total thickness of each multilayer is typically between 1000 and 2000 Å. Nominal thicknesses were confirmed by surface profilometry and low-angle x-ray reflectivity measurements. X-ray reflectivity measurements were performed in a Philips system with a 4-crystal Bartels Ge monochromator in the 220 configuration and Cu K_α radiation ($\lambda=1.540\,597$ Å); x-ray diffraction analyses were carried out with an automated Nicolet–Stöe L11 powder diffractometer using Cu K_α radiation. θ–2θ scans were taken to measure the specular reflection signal. In the diffuse geometry, the direction of the detector is fixed at 2θ, corresponding to the position of the first-order superlattice peak, while the incident angle of the x-ray beam is varied, giving a scan of reflected x-ray intensity as a function of the in-plane component of the scattering vector (rocking scan or ω scan).

The magnetization was measured at room temperature using a vibrating sample magnetometer operating at 85 Hz with a resolution of better than 10^{-4} emu. A number of zero-field cooled (ZFC) and field cooled (FC) magnetization and ac susceptibility runs were made using a modified Quantum Design Model 6000 Physical Property Measurement System.

Ion-beam irradiation at normal incidence was performed at a pressure near 10^{-7} Torr with 1 MeV Si^+ ions rastered over an area of 2.5×2.5 cm^2 using the Université de Montréal Tandetron accelerator. To avoid sample heating during irradiation, the beam current was kept below 0.1 $\mu A\,cm^{-2}$ and the samples were placed in thermal contact with a copper block maintained at 77 K. The dose Φ was systematically increased from an initial value of $10^{13}\,cm^{-2}$ to a final value of $3\times10^{16}\,cm^{-2}$ which results in about 0.1–30 displacements per atom (dpa) as estimated by transport of ions in matter (TRIM) simulations.[9] At each stage, the irradiation was performed simultaneously on the $\mathrm{Co}_{50}/\mathrm{Cu}_{75}$ multilayer and on reference $\sim$1000 Å Co and $\sim$1500 Å Cu films, also deposited on oxidized Si (100) substrates. The ion energy of 1 MeV was selected such that the projected ion range was much larger than the total film thicknesess (about 1750 Å); consequently, a uniform mixing profile throughout the multilayer is expected. TRIM simulations show that the energy loss of the 1 MeV Si^+ in a multilayer with thickness around 1000 Å is less than 200 keV (projected ion range of 1.5 μm) and that only a very small fraction (<0.1%) of the implanted ions remain within the magnetic films, the rest being transmitted or backscattered. Several of the irradiated multilayers were annealed at 250 °C for 2 h in a vacuum of 1×10^{-5} Torr.

III. IRRADIATION OF Co/Cu MULTILAYERS WITH THIN LAYERS

Intermixing induced by ion beams has been observed for many multilayers[10] but is by no means the only effect induced by ion irradiation. Other effects, such as local defects, demixing, or phase segregation may also play important roles. The relative importance of these effects depends on many factors such as ion mass, ion energy, dose, temperature, and the nature of the system. For example, while ion-beam mixing has been observed for many binary systems with negative heat of mixing, it has also been found that for systems with very large positive heat of mixing (e.g., Co/Ag), the two constituents segregate completely upon ion-beam bombardment.[11]

Due to their moderately large positive mixing heat ($\sim+13$ kJ/g)[12] Co and Cu are strongly immiscible and no equilibrium phases exist in the Co–Cu binary diagram.[13] However, with nonequilibrium techniques such as evaporation,[14] melt spinning,[15] and low-temperature co-deposition,[16] metastable CoCu alloys with extended solu-

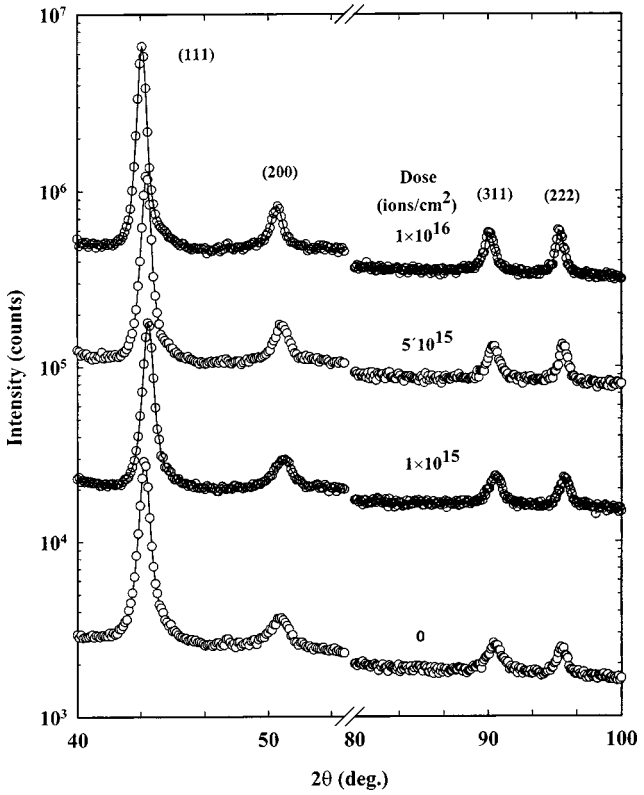

FIG. 1. High-angle x-ray diffraction spectra for a [Co(5 Å)/Cu (17 Å)]×50 multilayer: (a) as-deposited, (b) after irradiation at 1×10^{15} ions/cm^2, (c) after irradiation at 5×10^{15} ions/cm^2, and (d) after irradiation at 1×10^{16} ions/cm^2.

bility are attainable. The magnetic properties of such alloys have been reported.[16]

The question thus arises whether ion-beam bombardment can produce similar CoCu alloys. To investigate this possibility, a series of [Co(t Å)/Cu(17 Å)]×50 multilayers with t ranging from 2.5 to 12.5 Å has been grown and subjected to 1 MeV Si^+ ion irradiation at 77 K with ion doses up to 1×10^{17} ions/cm^2. The Co layers were chosen to be very thin in order to achieve steady mixing states at relatively low ion doses. The rest of this section will be devoted to a comparison of the structural and magnetic properties of such multilayers before and after irradiation at various ion doses.

A. High-angle x-ray diffraction

High-angle x-ray diffraction spectra of a [Co(5 Å)/Cu(17 Å)]×50 multilayer at different ion doses are plotted in Fig. 1. The as-deposited multilayer is principally textured in the fcc (111) direction; other fcc peaks, such as (200), (311), and (222) are also visible but much weaker. Since the region between 55° and 75° is dominated by substrate (Si) peaks, it has been omitted from the figure. It is interesting to note that, upon irradiation, no evident change is observed in either the intensities or the linewidths of the peaks, which precludes significant grain growth induced by the ion beam. The relative intensities between the peaks are also essentially unaffected and the film maintains a high degree of texture in the fcc (111) direction. At all doses, the Bragg peaks are sharp and well defined, indicating that significant lattice coherence remains upon irradiation. This observation can be ascribed to the fact that the lattice constants of fcc Co and fcc Cu are very close. Finally, irradiation at relatively low ion doses ($<5\times10^{15}$ ions/cm^2) shifts the peaks toward higher angles. This behavior might be explained by the mixing of Co into Cu that slightly reduces the average lattice constant of the Cu matrix. Irradiation at high doses ($>1\times10^{16}$ ions/cm^2), on the other hand, shifts the peaks toward lower angles. The exact reason for such a shift is still not clear, but can be understood in terms of the voids and inclusions produced by the implantation, as suggested by Schelp *et al.*[17] Noticeably, however, all these peak shifts are extremely subtle.

The above observation confirms that, over a wide dose range, the crystallographic changes induced by 1 MeV Si^+ ion irradiation on the Co/Cu system are small, in sharp contrast to the changes generated by many other techniques, such as deposition temperature or co-deposition, and reveals one of the major advantages of ion-beam irradiation as a tool to investigate the correlation between interface structure and GMR. With the morphology unchanged under irradiation, any change in the GMR of a multilayer can be ascribed to the variation of the interface structure.

B. Magnetic properties

Owing to the coherency of the Co and Cu lattices, high-angle x-ray diffraction has limited effectiveness for investigating intermixing or the existence of very small Co clusters dispersed in Cu matrix. On the other hand, magnetic properties of Co–Cu films have been found to be very sensitive to the atomic distribution of Co.[18] Depending on the sizes and the separations of the Co particles, the Co–Cu system may exhibit ferromagnetic, paramagnetic, superparamagnetic, or spin-glass behaviors. As a result, the magnetic properties of this heterogeneous system provide valuable information about its atomic structure.

Figure 2(a) presents the magnetization curves of the [Co(5 Å)/Cu(17 Å)]×50 multilayer measured at 300 K at ion doses up to 5×10^{15} ions/cm^2. Before irradiation, a large part of the magnetization saturates at very low magnetic field (<50 Oe), indicating that the Co layers are continuous or consist of islands with large lateral sizes. A small tail of the magnetization, that saturates at relatively high field, is also observed, arising from a small fraction of the multilayer that is antiferromagnetically coupled, or a small number of Co clusters coexisting with the continuous Co layers. Upon irradiation, two major features of the magnetization remain unchanged: first, all the magnetization curves exhibit marked hysteresis; second, all the magnetization curves are well saturated at a magnetic field of 1 kOe. For all ion doses, no sign of superparamagnetic behavior is observed, so that a significant presence of small Co clusters can be ruled out. The most noticeable effect of ion irradiation on the magnetization is the reduction in saturation level which decreases progressively with ion dose to 10% of the as-deposited value at 300 K.

For comparison, the corresponding magnetization curves of the same multilayer measured at low temperature (50 K) are shown in Fig. 2(b). Although ion irradiation produces

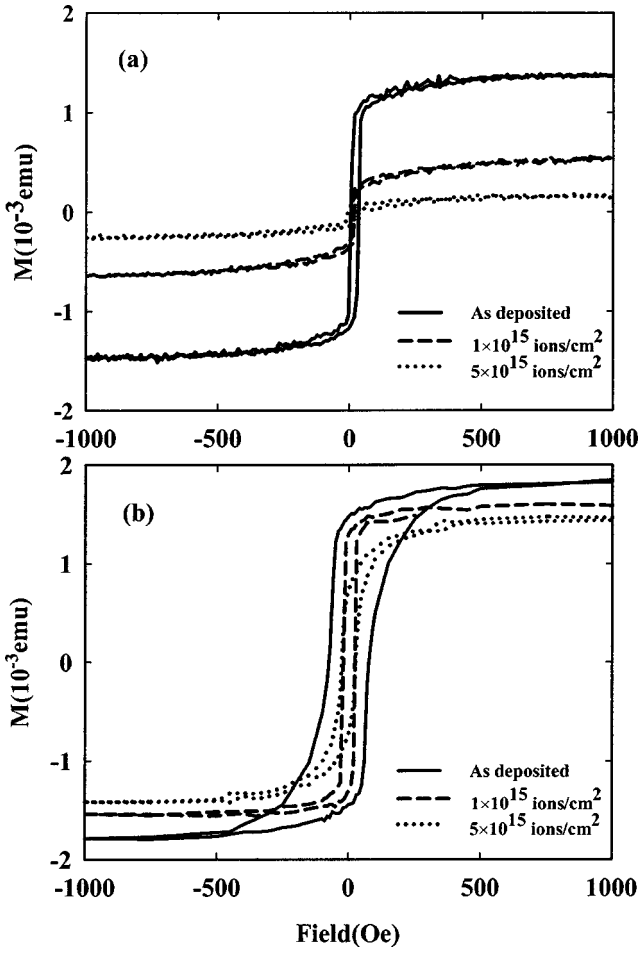

FIG. 2. Magnetization curves of [Co(5 Å)/Cu(17 Å)]×50 multilayers measured at (a) 300 K and (b) 50 K before irradiation (solid line), after irradiation with a dose of 1×10^{15} ions/cm^2 (dashed line), and with a dose of 5×10^{15} ions/cm^2 (dotted line).

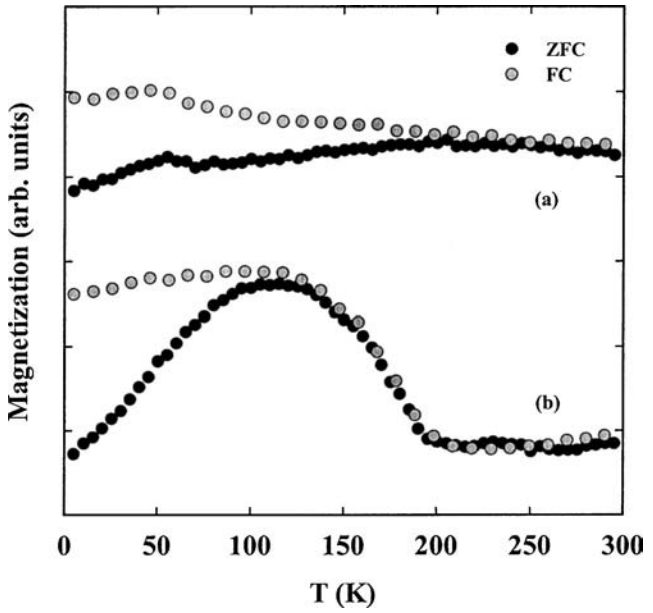

FIG. 3. The zero-field-cooled curves (ZFC) and field-cooled (FC) curves, with the external magnetic field $H_{ext}=20$ Oe, for [Co(5 Å)/Cu (17 Å)]×50 multilayer (a) as-deposited and (b) after irradiation with a dose of 5×10^{15} ions/cm^2.

significant changes in the magnetic remanence and coercivity of the multilayer, in contrast to the room temperature results, the saturation magnetization is only slightly reduced by irradiation. Such a contrast strongly suggests that the irradiation with ion dose of 5×10^{15} ions/cm^2 has reduced the magnetic transition temperature to between 50 and 300 K.

To investigate this effect, the magnetization of the multilayer has been measured as a function of temperature from 5 to 300 K, at an external field of 40 Oe. The results are shown in Fig. 3. For the as-deposited multilayer [Fig. 3(a)], both ZFC and FC data show little variation with temperature, which is characteristic of continuous Co layers or large Co particles with a Curie temperature well above 300 K. However, after irradiation at a dose of 5×10^{15} ions/cm^2 [Fig. 3(b)], the FC and ZFC curves drop sharply when the temperature is raised about 100 K, indicating a Curie transition around 190 K. In fact, the temperature dependence of the magnetization for the irradiated multilayer has been found to be very close to that of CoCu alloys with similar compositions obtained by low temperature co-deposition.[16] Furthermore, the Curie temperature estimated above is also consistent with the magnetic phase diagram of fcc CoCu alloy.[16] Such an agreement points to the conclusion that metastable CoCu alloys can be formed by low temperature irradiation with 1 MeV Si^+ ions. The main difference between the magnetic behavior of the irradiated Co/Cu multilayer and that of a co-deposition alloy lies in the absence of a spin-glass transition at low temperature for the multilayer. We suggest that such a difference is connected to the fact that small amounts of dispersed Co particles remain ferromagnetic at low temperatures. The existence of such Co particles in a heavily irradiated multilayer is indicated by the residual magnetization at room temperature.

In order to investigate how the magnetic moment depends on the Co concentration in ion-beam prepared CoCu alloys, a series of Co/Cu multilayers with various nominal average compositions and very thin layers (<15 Å) were deposited and were irradiated at a high ion dose of 10^{17} ions/cm^2. For these multilayers, low-angle x-ray reflectivity measurements have confirmed that the compositional modulation is completely destroyed at an ion dose of 5×10^{15} ions/cm^2. Moreover, the saturation magnetization (M_s) of these multilayers changes only slightly with increasing ion dose above 5×10^{16} ions/cm^2. Thus, it is expected that an ion dose level as high as 10^{17} ions/cm^2 should lead to a steady state of intermixing. In Fig. 4, the normalized magnetic moment (M/M_{bulk}) is shown as a function of nominal Co concentration, where M is the magnetic moment per Co atom for a heavily irradiated multilayer and M_{bulk} is the bulk magnetic moment of Co as estimated from a 1000 Å Co film. For a nominal composition smaller than about 25% Co, the mixed films are nonmagnetic at room temperature. The magnetic moment then increases with increasing Co concentration, and for nominal composition greater than about 50% Co, the average Co magnetic moment in the irradiated films is only slightly (~10%) smaller than the bulk value. These data are particularly useful in estimating the interfacial mix-

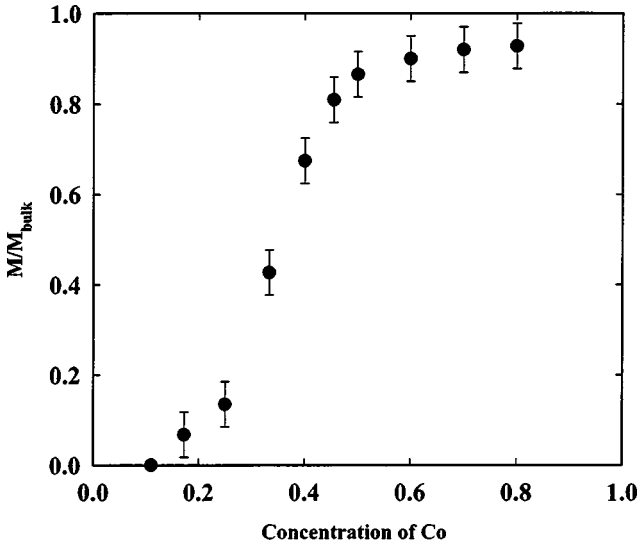

FIG. 4. Normalized magnetization (M/M_{bulk}) at 300 K of a series of $[\text{Co}(t_{\text{Co}}<15\ \text{Å})/\text{Cu}(t_{\text{Cu}}<15\ \text{Å})]\times 50$ multilayers as a function of nominal Co concentration $[t_{\text{Co}}/(t_{\text{Cu}}+t_{\text{Co}})]$ after irradiation at 1×10^{17} ions/cm^2. M_{bulk} is the bulk magnetic moment of Co obtained from a 1000 Å pure Co film.

ing width induced by ion irradiation, as will be discussed in Sec. IV.

IV. IRRADIATION OF Co/Cu MULTILAYERS WITH THICK LAYERS

A. High-angle x-ray diffraction

Figure 5 presents high-angle x-ray diffraction spectra of a $[\text{Co}(50\ \text{Å})/\text{Cu}(75\ \text{Å})]\times 14$ multilayer before irradiation and after irradiation at various doses up to 1×10^{16} ions/cm^2 (at which point the multilayer structure is destroyed as indicated by low-angle x-ray reflectivity measurements). The spectrum of the as-deposited multilayer is highly textured in the fcc (111) direction with a small fcc (200) components. The fcc (111) peak of the multilayer is located at $2\theta=43.9°$ between the (111) peak of fcc Cu (at 43.3°) and that of fcc Co ($2\theta=44.2°$). Two satellite peaks ($2\theta=42.8°$ and $2\theta=44.4°$, respectively) due to superlattice modulation are visible in the vicinity of the (111) Bragg peak. Their intensity is very weak due to the small lattice mismatch between fcc Co and fcc Cu. However, the positions of the peaks agree well with the period of the superlattice (~125 Å). The appearance of the satellite peaks, resulting from both the structural coherence on an atomic scale and a well-defined interface structure, further confirms the good quality of the multilayer.

In Fig. 5, the most noticeable effect of ion irradiation is the progressive reduction in the superlattice satellite peaks with increasing ion dose, in agreement with the picture that the interfaces are systematically blurred by ion mixing. At 1×10^{16} ions/cm^2, the satellite peaks are almost invisible. However, since the satellite peaks are rather weak even for the as-deposited multilayer, fitting these spectra for quantitative information about the mixing width is not feasible.

Other effects are also visible. For example, at high doses ($>10^{15}$ ions/cm^2), the (111) linewidth is slightly reduced upon irradiation. This change might be related to subtle grain

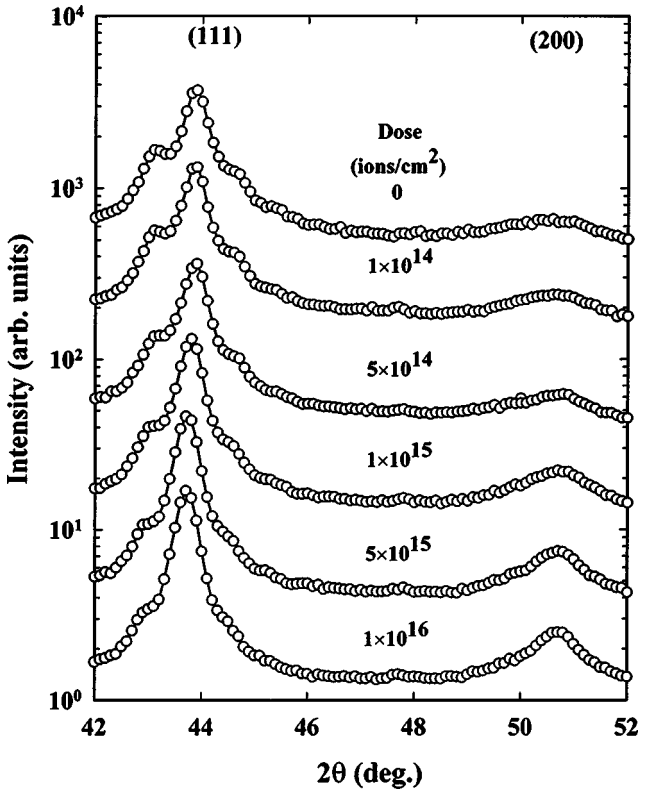

FIG. 5. High-angle x-ray diffraction spectra for the $[\text{Co}(50\ \text{Å})/\text{Cu}(75\ \text{Å})]\times 14$ multilayer as a function of ion dose.

growth due to the annealing of crystalline defects or grain boundaries during irradiation, as has been widely observed in other systems.[19] However, it should be noted that, due to the existence of satellite peaks, it is difficult to determine the variation in grain size (linewidth) precisely from these data. Also, upon irradiation, the (111) peak shifts slightly towards smaller angles. However, the corresponding change in average lattice constant is less than 1%, which is in contrast to the observations made for multilayers such as Au/Ni,[19] or Ag/Cu,[6] where pronounced shifts of the Bragg peaks upon irradiation have been recorded. Such a difference is not surprising, since neither the mixing of Co into the Cu matrix nor the mixing of Cu into the Co matrix is expected to change atomic spacing significantly. Again, the satellite peak intensity masks the exact position of the main Bragg peak, so that the precise peak shift cannot be determined reliably. Nevertheless, Fig. 5 shows that the changes in grain size or lattice constant are not considerable, especially at low doses.

Finally, at doses greater than 10^{15} ions/cm^2, the (200) peak is enhanced slightly. Such an effect, however, is hardly visible at low doses, and even at the largest dose ($>10^{16}$ ions/cm^2), a high degree of (111) texture is still maintained. Again, this observation in Co/Cu mulilayers is in contrast to many other multilayer systems with large lattice mismatches (for example, Au/Ni multilayers[19]). In those multilayers, ion-induced interdiffusion may reduce the lattice misfit and thus lattice strain, which favors the coherency between layers and consequently strongly improves the texture. In Co/Cu multilayers, this effect is not important given the fact that the lattice mismatch between Co and Cu is less than

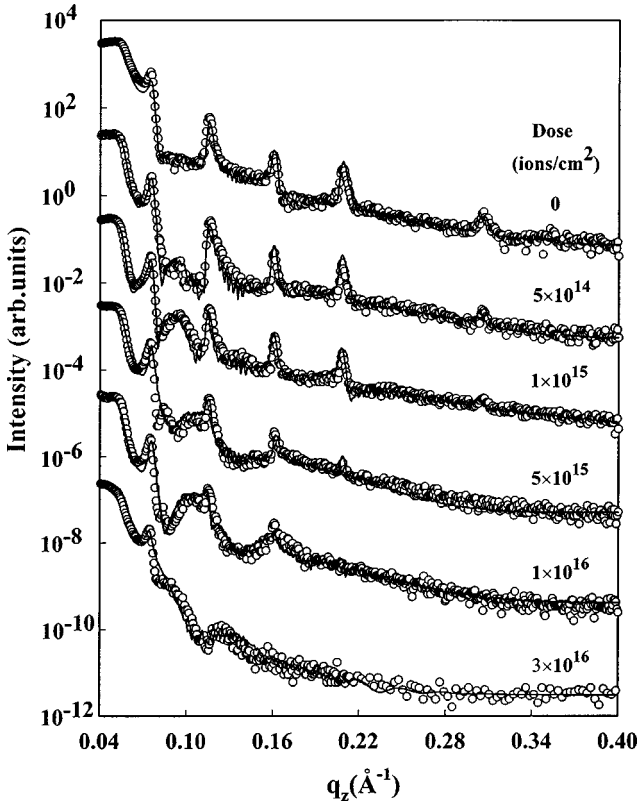

FIG. 6. Experimental (circles) and simulated (line) specular low-angle x-ray reflectivity spectra for a [Co(50 Å)/Cu(75 Å)]×14 multilayer at various ion doses.

2%, and film texture can simply be suppressed by ion-induced disorder.

B. Specular low-angle x-ray reflectivity

Figure 6. shows low-angle x-ray reflectivity spectra of the multilayer before and after irradiation at various doses. For the as-deposited multilayer, clear superlattice peaks are observed up to the sixth order, which confirms that the Co/Cu interfaces of the multilayer are well defined. Note that the peak of the fifth order is missing, which is expected from the 2:3 ratio between Co layer thickness and Cu layer thickness. Moreover, the composition wavelength of the multilayer (Co layer thickness+Cu layer thickness) can be determined by the positions of the superlattice peaks. Thus, the nominal thicknesses of the individual layers can be well confirmed.

Upon ion irradiation, the positions of the superlattice peaks remain the same, indicating the modulation period of the multilayer is not changed. On the other hand, the intensities of the superlattice peaks are progressively reduced as ion dose increases. At an ion dose of 3×10^{16} ions/cm^2, only a weak first-order peak is observed, signaling that the superlattice structure is almost completely destroyed. Given the fact that the intensities of the specular superlattice peaks are indications of interface sharpness and smoothness in a multilayer structure,[20] interface blurring induced by ion irradiation is clearly revealed by these measurements.

To quantify the effect of the ion irradiation, the x-ray spectra have been fitted with a standard optical model[21] (which is equivalent to dynamic calculations[22]), in which the x-ray reflectivity is calculated based on a matrix method. In this method, any single layer in a multilayer can be characterized by a matrix (2×2) as a function of layer thickness, the complex refractive index, and the wave vector of the incident beam. The multilayer matrix is obtained from the product of the matrices of individual layers.[23]

In order to include interfacial mixing, an error function composition profile at the interface is assumed, and is written as

$$C(x)=\frac{1}{2}+\frac{1}{2}\times\mathrm{erf}\left(\frac{x-x_0}{2\sqrt{Dt}}\right), \tag{1}$$

where $C(x)$ is the concentration of impurity atom at depth x, x_0 is the position of the original interface, and $2\sqrt{Dt}$ characterizes the amount of mixing at the interface. This interface profile is treated as a sequence of slices (~1 ML), each with constant composition. For the ith slice, the impurity concentration $c_i=C(x_i)$, where x_i is the depth of the slice in the vertical direction. The index of refraction of the slice is deduced from its average electron density and linear absorption coefficient, and is then applied to the appropriate matrix. The product of the matrices of the individual slices characterizes the entire interface region. For simplicity, a cutoff condition is introduced so that the slices with impurity concentration of less than 5% are treated as pure layers. We found that discarding such mixing tails has little effect on the fitting. In addition, a global roughness factor has also been incorporated into the calculation by assuming a Gaussian form (with a Debye–Waller factor). Model calculations are fitted to the data using a nonlinear least-squares procedure.[23] In all calculations, bulk values are used for electronic densities and absorption coefficients of Co and Cu. The modulation wavelength of the multilayer is obtained from the peak positions for the as-deposited spectrum, and is kept constant when calculating all spectra corresponding to various doses.

Although many parameters are involved in the fitting procedure, convergence to a unique set is obtained in each case. Parameters, such as thickness of an oxide overlayer (t_{oxide}) and its roughness (σ_{ov}) as well as the substrate roughness (σ_s), influence the overall profile of the reflectivity curves but have little effect on the intensities of superlattice peaks. Increasing σ_{ov} and σ_s leads to a faster decrease of the reflected intensity and to a reduction of the amplitude of the total thickness fringes as the scattering wave vector increases. As well, the presence of an oxide overlayer introduces extra oscillatory features for which the wavelength is inversely proportional to the layer thickness.

As shown in Fig. 6, the extra oscillation appears between the first- and second-order superlattice peaks at a dose of 1×10^{15} ions/cm^2, and corresponds to an overlayer of thickness 71±3 Å. Such an effect is commonly observed for intermediate ion doses, and can probably be ascribed to the damage made by the ion beam that promotes the diffusion of oxygen when the sample were used for successive transport and magnetic measurements. With further irradiation, this feature is shifted towards higher angles, indicating that the thickness of the overlayer decreases. As well, the overall

profile of a spectrum is hardly changed upon irradiation (except for the highest dose). This behavior indicates that the overlayer roughness is not changed with ion dose. From our fittings, this roughness is estimated to be around 15 Å. In order to explain the extra oscillatory features induced by the ion beam, the oxide overlayer, whose thickness varies with ion dose, has to be considered.

Both interface mixing width and interface roughness suppress the superlattice peak intensities. Unfortunately, in specular measurements, their effects are rather similar and therefore it is difficult to distinguish interfaces that are truly diffuse from those which contain genuine roughness. However, as suggested by Savage *et al.*,[24] this problem can be partially solved by decomposing the interface roughness into two parts

$$\sigma^2 = \sigma_c^2 + \sigma_u^2, \tag{2}$$

where σ is the total rms roughness, σ_c corresponds to the contribution from roughness being correlated between layers, and σ_u corresponds to the contribution from the random roughness with high frequency and short lateral correlation scale.

The correlated roughness typically has a large lateral correlation length, while uncorrelated roughness may not be strictly distinguishable from intermixing (which is commonly regarded as random roughness with a lateral correlation length shorter than 15 Å[25]). Based on this assumption, we treat the uncorrelated part of the interface roughness as a constant for all spectra, while any actual change of such roughness upon irradiation is incorporated into the interface mixing. As will be discussed in the next section, the correlated part of interface roughness is obtained from the diffuse scattering measurements around superlattice peaks, and thus can be well separated from interface mixing.

The calculated curves are shown as solid lines in Fig. 6 where it is seen that the agreement between experimental and calculated curves with respect to both the position and the intensity of the peaks is excellent for all ion doses. The structural parameters extracted from the fittings are listed in Table I for the as-deposited and irradiated samples.

Fitting the spectra using the model described, the interface mixing width is obtained as a function of ion dose and is plotted in Fig. 7. Up to an ion dose of 1×10^{16} ions/cm^2, the square of the ion-beam mixing width ($4Dt$) varies linearly with ion dose, as predicted by the cascade model of ion-beam mixing. For the spectrum with the highest dose (3×10^{16} ions/cm^2), the mixing width exceeds the thickness of the Co layer, and the above analysis breaks down. From Fig. 7, the ion beam mixing efficiency $d(4Dt)/d\phi$ is obtained to be about 400 Å.[4] This can be compared with the theoretical value calculated using the formula developed by Sigmund and Gras-Marti for ballistic ion-beam mixing[26] which is in the form

$$\frac{d(4Dt)}{d\Phi} = \frac{2}{3}\Gamma_0 \xi \frac{F_D R_c^2}{\rho E_d}, \tag{3}$$

where $\Gamma_0 = 0.608$, $\xi = [4m_1m_2/(m_1+m_2)^2]^{1/2}$ where m_1 and m_2 are the masses of the atoms involved in collisions; R_c is the mean-square range of a displaced atom taken to be 1 nm, and E_d is the average minimum displacement energy; ρ is the average atomic density and F_D is the energy deposited per unit path length at the interface. Taking $E_d = 21$ eV (the average of Co and Cu[27]), and $F_d = 35$ eV/Å (as obtained from TRIM simulations), Eq. (5.4) predicts a mixing efficiency of 794 Å.[4] This value is comparable to that obtained from our x-ray reflectivity fitting, suggesting that the ballistic mixing is the principal mixing mechanism of the multilayers at low temperature. The difference between theoretical and experimental values of mixing efficiency may be related to thermal spike effects which reduce the mixing efficiency in an immiscible system.

TABLE I. Structural parameters extracted from the fitted results shown in Figs. 2 and 4 for a [Co(50 Å)/Cu(75 Å)]×14 multilayer at various ion doses. $2\sqrt{Dt}$ characterizes the ion mixing width, as defined in Eq. (1), σ_I, the overall interface roughness; σ_c, the correlated part of interface roughness; σ_o, the oxide overlayer roughness; t_o, the oxide overlayer thickness; and ξ, lateral roughness correlation length.

Dose (ions/cm^2)	$2\sqrt{Dt}$	σ_I (Å)	σ_c (Å)	t_o (Å)	ξ (Å)	σ_o (Å)
0	0	6.10	1.56	17.3	450	14.7
					0	
5×10^{14}	3.8	6.02	1.20	22.4	310	15.5
					0	
1×10^{15}	6.5	6.08	1.48	71.0	300	15.8
					0	
5×10^{15}	14.5	6.32	2.26	60.5	235	15.9
					0	
1×10^{16}	20.2	6.51	2.75	60.7	160	16.7
					0	
3×10^{16}	41.8	10.1	8.20	33.6	150	20.2
					0	

C. Diffuse low-angle x-ray reflectivity

Nonspecular reflectivities from x-ray scattering measurements contain information about the magnitude and lateral

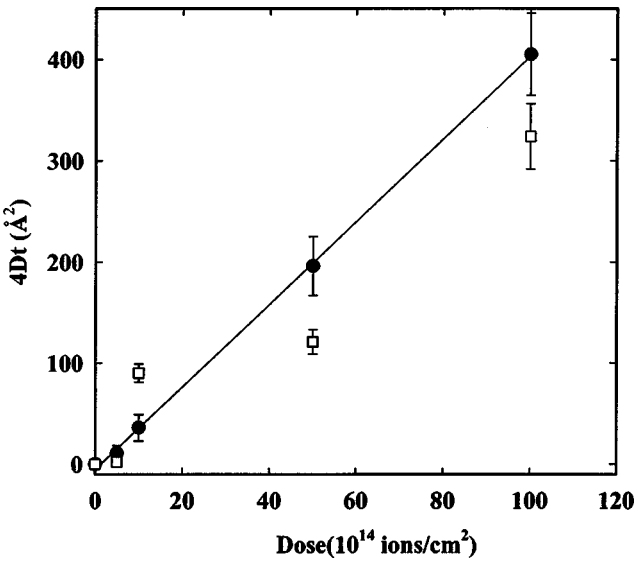

FIG. 7. The square of the mixing width ($4Dt$) as a function of ion dose obtained from fitting to specular low-angle x-ray reflectivity data (●) and to saturation magnetization measurements ( ).

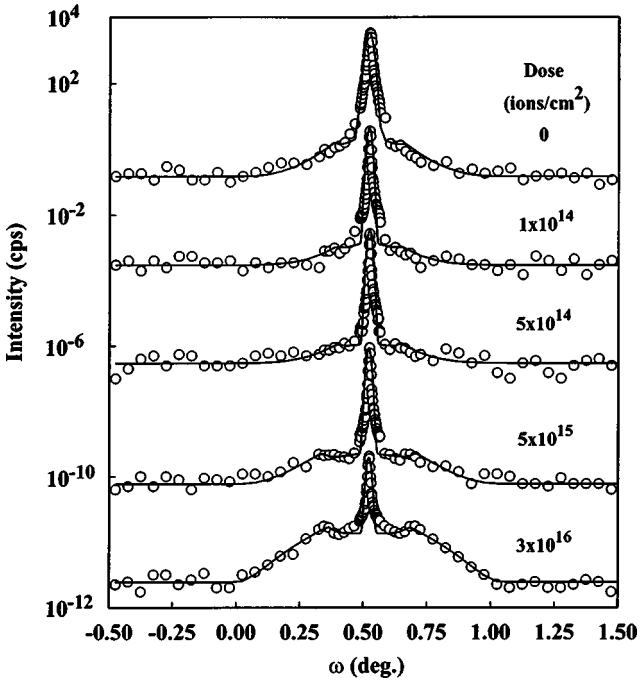

FIG. 8. Experimental (circles) and simulated (line) diffuse low-angle x-ray reflectivity spectra for a [Co(50 Å)/Cu(75 Å)]×14 multilayer as a function of ion dose.

(height–height) correlation length of correlated roughness. Figure 8 shows the results of rocking scans around the first-order superlattice peak for the $Co_{50}Cu_{75}$ multilayer before irradiation and after irradiation at various doses. For the as-deposited multilayer, the spectrum consists of a central spike arising from specular scattering, and a relatively weak and slowly varying diffuse background in its vicinity. Irradiation at low doses slightly reduces the background, suggesting the layers became smoother. For ion doses larger than 5×10^{14} ions/cm^2, the diffuse signal systematically increases with ion dose. At high doses, the so-called ''Yoneda wings'' (broad maxima corresponding to critical angle after which the diffuse intensity drops rapidly) are clearly seen. Such observations indicate an increase in interface roughness induced by ion irradiation. In addition, the shape of the diffuse background also varies with ion dose, which suggests changes of average roughness correlation length upon ion irradiation.

The diffuse scattering intensity can be fitted using the model initially developed by Sinha *et al.*[28] for a single rough surface and later extended to multilayer structures by Savage *et al.*[24] Assuming that for two points on a surface separated by distance $R=(X^2+Y^2)^{1/2}$, the correlation function

$$C(X,Y)=\sigma^2\exp[-(R/\xi)]^{2h} \tag{4}$$

is obtained, in which ξ is the lateral roughness correlation length, h (Hurst parameter) is related to the fractional dimension and is close to 1/2 for Co/Cu multilayers.[25] Using this correlation function, and supposing that the intensity of the scattered x rays is detected through a sufficiently long slit along X direction, the scattered intensity is written as

$$I(q_x,q_z)=2\pi I_0\exp(-q_z^2\sigma_c^2)/q_z^2\left[2\pi\delta(q_x)+\sum_{m=1}^{\infty}\frac{2\xi(q_z^2\sigma_c^2)^m}{m(m!)}\frac{1}{(1+q_x^2\xi^2/m^2)}\right], \tag{5}$$

where q_x, q_z are the in-plane and vertical components of the scattering vector, respectively, σ_c is the correlated roughness. The intensity in Eq. (5) is separated into a δ function corresponding to the specular central spike in Fig. 7 and a diffuse component. The intensity calculated from Eq. (3) is then multiplied by $\sin\omega/\sin\theta$, which corrects the asymmetry effect resulting from the change in the volume of the specimen being probed, as well as an envelope function that corrects for two geometrical effects,[24] and finally is convoluted with a function representing the instrumental broadening.

In Fig. 8, the rocking curves at various ion doses are fitted using Savage's model described above. It should be mentioned that Savage's model is based on the Born approximation under which the Yoneda wings cannot be reproduced. To reproduce Yoneda wings, distorted-wave Born approximation (DWBA) has to be used to refine the Savage model. As shown by Sinha *et al.*,[28] the main effect of introducing DWBA is to introduce a prefactor $|T(k_1)|^2|T(k_2)|^2$ to the scattering intensity calculated from the Born approximation. Here k_1 is the wave vector of the incident x ray, $-k_2$ is the time reversed state for the incident beam. $T(k)$ is the transmission coefficient of x ray with incident wave-vector k, and can be calculated from Fresnel theory. This prefactor from DWBA is introduced into our calculations to simulate diffuse scattering near critical angles. Solid lines in Fig. 8 present the fitted curves. As can be seen, all rocking curves are well reproduced by our calculations. The interface roughness and its lateral correlation length obtained from our fitting are plotted in Fig. 9, as well as listed in Table I, as functions of ion dose. Upon initial irradiation, the correlated interface roughness decreases slightly from 1.6 Å to a value of 1.2 Å at 5×10^{14} ions/cm^2. At higher doses, the interface roughness continuously increases, reaching 8.2 Å at a dose of 3×10^{16} ions/cm^2. As mentioned in the previous section, such variation of the correlated roughness with ion irradiation has been taken into account when fitting specular spectra. It should also be noted that, except for the highest dose, the range of variation of correlated roughness is within about 2 Å, and thus should not have significantly affected the fitting to the specular spectra. Also shown in Fig. 9, the lateral coherence length is about 4500 Å before irradiation, which is close to that obtained by de Bernabé *et al.*[25] in their Co/Cu multilayers. This large correlation length typically reflects good diffusion during film growth. As the ion dose increases, the average lateral coherence length decreases monotonically to about 1500 Å at a maximum ion dose of 10^{16} ions/cm^2.

D. Saturation magnetization (M_s)

Intermixing between Co and Cu in Co/Cu multilayers forms magnetically inactive regions and leads to a decrease in the saturation magnetization (M_s).[29] Therefore, measuring M_s as a function of ion dose provides another probe to study

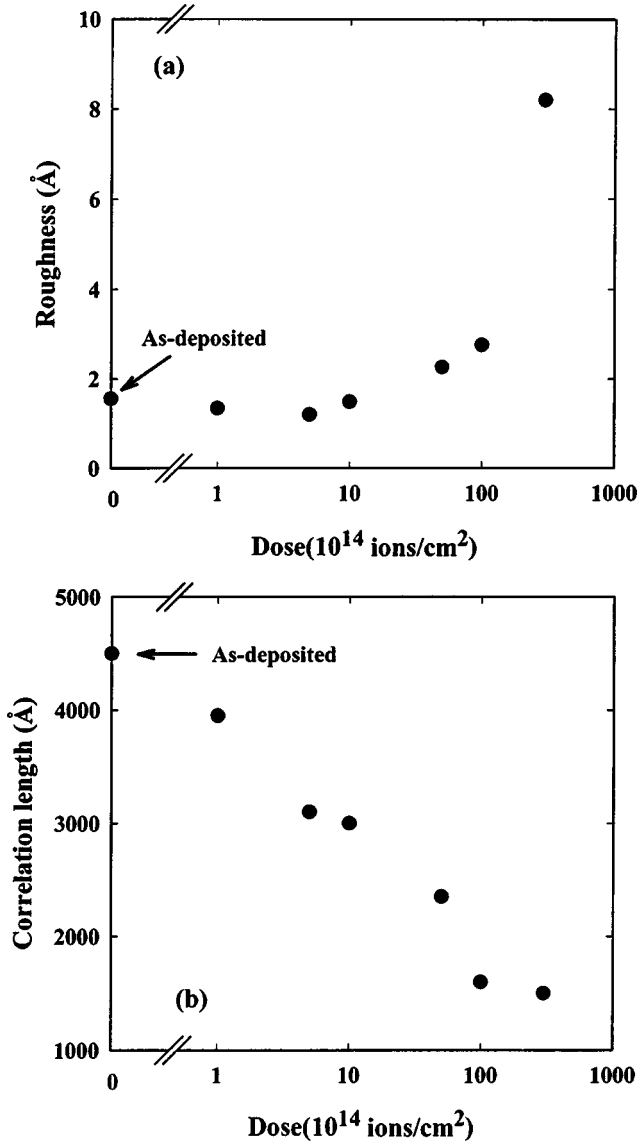

FIG. 9. (a) Interface roughness and (b) roughness lateral correlation length as functions of ion dose obtained from diffuse low-angle x-ray reflectivity spectra fitting.

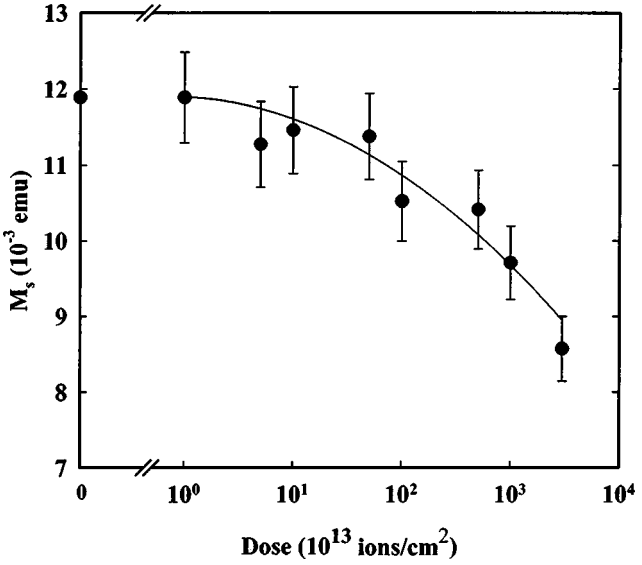

FIG. 10. Saturation magnetization of a [Co(53 Å)/Cu(76 Å)]×15 multilayer as a function of ion dose: (●) represent experimental data, and the continuous line represents calculated values using the mixing widths obtained from fitting to the specular low-angle reflectivity data.

the mixing effect induced by ion-beam bombardment in such a magnetic/nonmagnetic structure. The results of our measurements are shown in Fig. 10. As can be seen, a decrease of M_s is observed for ion doses above 10^{15} ions/cm^2, falling approximately 20% at a dose of 3×10^{16} ions/cm^2. This variation provides clear evidence that intermixing has been induced by ion-beam irradiation.

The intermixing width can be estimated from these data: first, an error function composition profile is introduced at each interface, the same as used in modeling small-angle x-ray reflectivity fitting, then, this interface region is divided into many thin slices (~1 ML) and the average composition of each slice is calculated from the error function; finally, the total M_s of the multilayer is evaluated by summing up the contributions of all slices

$$M_s = \sum m(c_i) n_i , \tag{6}$$

where n_i is the number of Co atoms in the ith slice, c_i is the Co concentration in the ith slice, and $m(c_i)$ is the average magnetic moment per Co atom related to the cobalt concentration.

To estimate $m(c)$, a series of Co/Cu multilayers with various nominal compositions and very thin layers [Co(t_{Co} <15 Å)/Cu(t_{Cu}<15 Å)] were deposited and then irradiated at a high ion dose of 10^{17} ions/cm^2. For such multilayers, x-ray reflectivity measurements have confirmed that any compositional modulation is completely destroyed at an ion dose of 5×10^{15} ions/cm^2. Moreover, M_s of these multilayers change only slightly with increasing ion dose above 2×10^{16} ions/cm^2. Thus, it is expected that an ion dose level as high as 10^{17} ions/cm^2 should lead to a steady state of intermixing.

Using this approach, it is possible to compare the results from x-ray and magnetic measurements. The solid line in Fig. 10 shows the dependence of M_s on ion dose calculated from the ion-mixing width obtained from x-ray reflectivity fitting. The result agrees with the experimental data. Similarly, M_s measured from experiments can be used to estimate this width at various doses with Eq. (6). The results are shown in Fig. 7. As can be seen, the ion-beam mixing width extracted from x-ray reflectivity measurements and magnetic measurements are consistent.

V. CONCLUSIONS

The structural modification in Co/Cu multilayers by 1 MeV Si^+ ion irradiation at 77 K has been analyzed by various x-ray scattering techniques. Low-angle x-ray specular reflectivity measurements are shown to be a sensitive tool to probe ion-beam mixing effects on an angström scale in these multilayers. Fitting to the reflectivity spectra using a matrix method yields a mixing efficiency comparable to that predicted by the ballistic cascade mixing model. The ion-beam

mixing widths obtained from such fitting are consistent with the values estimated from magnetic measurements. Off-specular x-ray reflectivity measurements reveal a nonmonotonic variation of correlated interface roughness and a progressive decrease in the average lateral roughness correlation length with increasing ion dose.

Structural analysis and magnetization measurements presented in this article point to the conclusion that at high ion doses, irradiating Co/Cu multilayers generates metastable Co–Cu alloys, whose electrical and magnetic properties have been found to be very similar to the Co–Cu alloys, fabricated by other nonequilibrium methods. At low ion doses, ion-beam irradiation of Co/Cu multilayers generates interfacial mixing of short range with no significant effects on other structural properties such as grain size or film texture. As a result, it is possible to isolate the effects of interface structure on the magnetic and magnetotransport properties. In Paper II,[8] we show that, indeed, the GMR and antiferromagnetic coupling depend strongly on the ion-beam short range interfacial mixing. The mixing efficiency obtained from this study will be used in order to correlate the transport, namely GMR, and magnetic coupling with the interface structural changes introduced by ion-beam irradiation in Co/Cu multilayers with large GMR ratios.

ACKNOWLEDGMENTS

The authors would like to thank M. Sutton (McGill) for valuable assistance with the modeling of the XRR data, L. Cheng (McGill) for help with x-ray diffraction measurements. It is also a pleasure to acknowledge P. Bérichon and R. Gosselin for the operation of the tandem accelerator and assistance during the ion irradiation experiments. This research has received financial support from the Natural Sciences and Engineering Research Council of Canada and the Fonds pour la formation de chercheurs et l'aide à la recherche du Quebec.

[1] M. N. Baibich, J. M. Broto, A. Fert, F. Nguyen Van Dau, F. Petroff, P. Etienne, G. Creuzet, A. Friederich, and J. Chazelas, Phys. Rev. Lett. **61**, 2472 (1988).
[2] S. S. P. Parkin, in *Ultrathin Magnetic Structures II*, edited by B. Heinrich and J. A. C. Bland (Springer, Berlin, 1994).
[3] D. M. Kelly, I. K. Schuller, K. Korenivski, K. V. Rao, K. K. Larsen, J. Bottinger, E. M. Grorgy, and R. B. van Dover, Phys. Rev. B **50**, 3481 (1994).
[4] K. Temst, G. Verbanck, R. Schad, G. Gladyszewski, and M. Hennion, Physica B **234–236**, 467 (1993).
[5] M. Cai, T. Veres, S. Roorda, R. W. Cochrane, R. Abdouche, and M. Sutton, J. Appl. Phys. **81**, 5200 (1997).
[6] L. C. Wei and R. S. Averback, J. Appl. Phys. **81**, 613 (1997).
[7] G. Gladyszewski, Thin Solid Films **204**, 473 (1991); L. F. Schelp, M. Carara, A. D. C. Viegas, M. A. Z. Vasconcellos, and J. E. Schmidt, J. Appl. Phys. **75**, 5262 (1994).
[8] M. Cai, T. Veres, S. Roorda, F. Schiettekatte, and R. W. Cochrane, J. Appl. Phys. **95**, 2006 (2004).
[9] J. F. Ziegler and J. P. Biersack, *The Stopping and Range of Ions in Solids* (Pergamon, New York, 1985).
[10] Y. T. Cheng, Mater. Sci. Rep. **5**, 47 (1990).
[11] T. Veres, M. Cai, S. Germain, M. Rouabhi, F. Schiettekatte, S. Roorda, and R. W. Cochrane, J. Appl. Phys. **87**, 8513 (2000).
[12] A. R. Miedema, Philips Tech. Rev. **36**, 217 (1976).
[13] M. Hansen, *Constitution of Binary Alloys* (McGraw–Hill, New York, 1958), p. 469.
[14] E. Kneller, J. Appl. Phys. **33S**, 1355 (1962).
[15] R. H. Yu, X. X. Zhang, J. Tejada, and J. Zhu, Phys. Rev. B **52**, R6987 (1995).
[16] J. R. Childress and C. L. Chien, Phys. Rev. B **43**, 8089 (1991).
[17] L. F. Schelp, M. Carara, A. D. C. Viegas, M. A. Z. Vasconcellos, and J. E. Schmidt, J. Appl. Phys. **75**, 5262 (1994).
[18] A. E. Berkowitz, J. R. Mitchell, M. J. Carey, A. P. Young, S. Zhang, F. E. Spada, F. T. Parker, A. Hutten, and G. Thomas, Phys. Rev. Lett. **68**, 3745 (1992).
[19] F. Tamsier, V. Jaouen, Ph. Guerin, and G. Gladyszewski, Thin Solid Films **275**, 247 (1996).
[20] For a review, see, e.g., E. Chason and T. M. Mayer, Crit. Rev. Solid State Mater. Sci. **22**, 1 (1997).
[21] M. Born and E. Wolf, *Priciples of Optics* (Pergamon, Oxford, 1964), p. 57.
[22] R. W. James, *The Optical Principles of Diffraction of X-rays* (Cornell University Press, New York, 1965).
[23] Y. Huai, R. W. Cochrane, and M. Sutton, Phys. Rev. B **48**, 2568 (1993).
[24] D. E. Savage, J. Kleiner, Y. H. Phang, T. Jankowski, J. Jacobs, R. Kariotis, and M. G. Lagally, J. Appl. Phys. **69**, 1411 (1991).
[25] A. de Barnabe, M. J. Capitan, H. E. Fischer, and C. Prieto, J. Appl. Phys. **84**, 1881 (1998).
[26] P. Sigmund and A. Gras-Marti, Nucl. Instrum. Methods **182–183**, 25 (1981).
[27] H. H. Anderson, Appl. Phys. **18**, 131 (1979).
[28] S. K. Sinha, E. B. Sirota, S. Garoff, and H. B. Stanley, Phys. Rev. B **38**, 2297 (1988).
[29] Y. Saito, J. Phys. Soc. Jpn. **62**, 1450 (1993).